Vol. 14, No. 1, 2023
ISSN 2233-4203/ e-ISSN 2093-8950
ARTICLE www.msletters.org | Mass Spectrometry Letters

Characterization of *in vitro* Metabolites of Methylenedioxy Designer Drugs

Jun Sang Yu[1,2], So Young Jo[1], Il-Ho Park[3], and Hye Hyun Yoo[1]*

[1]*Institute of Pharmaceutical Science and Technology and College of Pharmacy, Hanyang University, Ansan, Gyeonggi-do 15588, Korea*
[2]*Research Institute of Engineering & Technology, Hanyang University, Ansan, Gyeonggi-do 15588, Korea*
[3]*College of Pharmacy, Sahmyook University, 815, Hwarang-ro, Nowon-gu, Seoul, 01795 Republic of Korea*

Received February 10, 2023, Revised March 4, 2023, Accepted March 9, 2023
First published on the web March 31, 2023; DOI: 10.5478/MSL.2023.14.1.1

Abstract : Eutylone, dibutylone, and dimethylone are potential psychotropic designer drugs. The purpose of this study was to investigate the *in vitro* metabolic pathways of synthetic cathinones with methylenedioxy groups. The three methylenedioxy derivatives were incubated with human liver microsomes. The metabolites were characterized based on liquid chromatography and quadrupole-time-of-flight mass spectrometry. Eutylone, dibutylone, and dimethylone were metabolized to yield three, six, and four metabolites, respectively. Reduction and demethylenation were the major metabolic pathways for all three drugs tested. However, dibutylone and dimethylone showed an additional metabolite generated via N-oxidation. These results provide evidence for the *in vivo* metabolism of methylenedioxy synthetic cathinones, and could be applied to the analysis of synthetic cathinones and their relevant metabolites in biological samples.

Keywords : Methylenedioxy derivatives, Designer drug, Metabolism, LC/Q-TOF MS

Introduction

Synthetic cathinones, more commonly known as “bath salts”, are sympathomimetic drugs chemically related to cathinone, a stimulant found in khat plants.[1, 2] Cathinone is a monoamine alkaloid that is chemically similar to ephedrine, cathine, methcathinone, and other amphetamines, and consequently exhibits stimulant effects. Synthetic cathinones can change much more strongly than original products and as a result are, sometimes very dangerous.[3,4] Synthetic cathinones have been widely used in the drug market since the mid-2000s due to their characteristics, which are easy to discover using the internet. Due to the abuse potential of synthetic cathinones, many countries have been trying to regulate laws. However, synthetic cathinones have been newly synthesized to avoid legal control and to increase the stimulant effects.[5-7] As a result of expert evidence from the National Forensic Service, more than 20 kinds of new phenethylamine-like drugs have been detected in field evidence by police and prosecutors. Most of the detected substances are synthetic cathinone and amphetamine analogues.[8,9] Thus, as the abuse cases of new synthetic cathinone analogues have been increasing in recent years, the need for a confirmatory method of cathinone testing has emerged.

When drug users are arrested, they are usually examined through biological sampling. At this point, the parent drug can be analyzed and detected in the biological sample, and the presence of the metabolite in the sample can indicate whether or not the drug was used. Metabolite/drug ratios can sometimes provide estimates of metabolic change. To detect drugs in biological samples, the metabolic fate of the drugs should be studied. Several metabolism screening and confirmation methods have been published for the detection of synthetic cathinones in biological samples.[10-16]

Thus, the ideal analysis for detecting drugs is taking biological samples through drug clinical trials to identify metabolites. However, it is difficult to directly perform the clinical trial of illegal drugs such as synthetic cathinones because of conflict with forensic science. Therefore, *in vitro* metabolite study of synthetic cathinones is necessary to find a biomarker for evidence of drug abuse instead of the clinical trial.

Eutylone, dibutylone, and dimethylone belong to the methylenedioxy group, as their backbone is different from that of synthetic cathinone. As these are illegal drugs such

*Reprint requests to Hye Hyun Yoo
https://orcid.org/0000-0001-8282-852X
E-mail: yoohh@hanyang.ac.kr

as synthetic cathinones, identification of metabolites *in vitro* is needed. Thus, in this study, a metabolism study of eutylone, dibutylone, and dimethylone was conducted. The aim of this study is to identify their phase I metabolites in human liver microsomes using liquid chromatography/ quadrupole-time-of-flight mass spectrometry analysis.

Materials and methods

Chemicals and materials

Eutylone, dimethylone, and dibutylone were supplied by the National Forensic Service Center (Seoul, Korea). Glucose-6-phosphate, β-nicotinamide adenine dinucleotide phosphate (NADP), and glucose-6-phosphate dehydrogenase were purchased from Sigma Chemical Co. (St Louis, MO, USA). Pooled human liver microsomes, were purchased from BD Gentest Corp. (Woburn, MA, USA). Methanol, dimethyl sulfoxide (DMSO), and acetonitrile were purchased from Fisher Scientific (Fair Lawn, NJ, USA). All other chemicals were analytical grade.

Microsomal incubation

A stock standard solution of the drug was prepared at 10 mM in DMSO, respectively. The incubation mixtures consisted of 0.5 mg/mL human liver microsomes, 50 μM of the drug, and an NADPH-generating system (NGS; 0.1 M glucose-6-phosphate, 10 mg/mL $NADP^+$ and 1 U/mL glucose-6-phosphate dehydrogenase) using a total volume of 1000 μL potassium phosphate buffer (0.1 M, pH 7.4). Reactions were initiated by the addition of NGS after a 5-min pre-incubation at 37°C. Incubations were carried out for 0, 0.5, 1, 1.5, and 2 hours, and quenched by the addition of 100 μL of ice-cold 1% formic acid to the reaction mixture. The sample was vortex-mixed for 2 min and applied to the Waters OASIS HLB cartridges (Milford, MA, USA), which were activated with 1 mL of MeOH and equilibrated with 0.1% acetic acid. After sample loading, the cartridges were washed with 2 mL of 0.1% acetic acid (1 mL × 2) and eluted with 1 mL of MeOH. The elutes were dried under N_2 gas at 55°C and reconstituted with 100 μL of 10% mobile phase solvent B. Five microliter-aliquots were injected onto the LC-MS/MS system.

LC/QTOF MS analysis

The HPLC system consisted of an Agilent 1260 series binary gradient pump, a vacuum de-gasser, an autosampler, and a thermostatic column compartment with an Agilent 6530 quadrupole-time-of-flight (QTOF) mass spectrometer equipped with an electrospray ionization source (Agilent Technologies, Inc., Santa Clara, CA, USA). The column used for the separation was a Kinetex C18 (2.1 × 100 mm, 2.6 μm; Phenomenex, Torrance, USA). The HPLC mobile phases consisted of 0.1% formic acid and 0.1% trifluoroacetic acid in water (solvent A), and 90% acetonitrile in solvent A (solvent B). A gradient program was used with a flow rate of 0.3 mL/min. The initial composition of the organic phase (B) was 1.5%; this was increased to 15% in 20 min and again increased up to 95% in 1 min. It was then changed back to its initial condition over 1 min, followed by a 4 min re-equilibration. The total run time was 31 min. The entire column of elutes was directly introduced into an electrospray ionization (ESI) interface. Nitrogen was used as a nebulizing gas, sheath, and collision gas. The drying gas temperature was 300°C at 20 psi, and the sheath gas temperature was 350°C at a flow rate of 10 L/min. The mass spectrometer was operated in the positive ion mode with a 100-1000 *m/z* range, and at a 2 GHz extended dynamic range. For the product ion scan, the monitored mass range was 50-500 Da and the collision energy was set to 15 eV. Data were collected in a centroid format and processed with Mass Hunter software. Mass calibration was performed prior to the sample analysis using a calibration solution provided by the manufacturer. For each analysis, a calibrant solution containing purine (*m/z* 121.0509) and HP-921 (*m/z* 922.0098; Agilent) was delivered through an external isocratic pump as internal calibrants.

Results

In vitro metabolism of eutylone in human liver microsomes

Metabolites of eutylone in human liver microsomes were analyzed through LC-Q/TOF-MS. Three metabolites were identified with a mass accuracy of less than 5 ppm. Metabolites were eluted at 8.7, 15.3, and 17.4 min, with eutylone eluting at 18.8 min (Figure S1, A). The E-M1 was 12 Da lower than eutylone and corresponded to the demethylenation of eutylone. The molecular weight of E-M2 was 28 Da lower than eutylone. The E-M2 was postulated to be an N-dealkylation metabolite. The molecular weight of E-M3 was 2 Da higher than eutylone. The E-M3 was postulated to be a beta-keto reduction metabolite. The accurate mass data for the product ions of the metabolites are summarized in Table 1.

The chemical structures of the detected metabolites were explained by the fragmentation patterns (Figure S2). The structure of each metabolite was characterized by comparison with the MS/MS fragmentation patterns of the parent. The MS/MS analysis of protonated eutylone yielded a major product ion at *m/z* 218, 188, 161, and 86. The ion at *m/z* 218 resulted from the dehydration of eutylone, and the ion at *m/z* 86 resulted from the alpha-cleavage between positions 1 and 2. The ion at *m/z* 188 resulted from the loss of a dioxolane and *m/z* 161 corresponded to the loss of the amine group and demthylenation. The MS spectrum of E-M1 showed major product ions at *m/z* 206, 188, and 86. The ion at *m/z* 206 resulted from the dehydration of E-M1. The characteristic product ions at *m/z* 188 and 86 indicated the same product ion as their parent. The MS spectrum of E-M2 displayed major product ions at *m/z* 190, 160, 149, and 132. The ions at *m/z* 190 indicated the loss of water.

Table 1. Accurate mass data for the product ions of synthetic cathinone derivatives and their metabolites.

Name	RT	Proposed elemental composition	Exact mass $[M+H]^+$	Measured mass $[M+H]^+$	Error (ppm)
Eutylone	18.8	C13H17NO3	236.1281	236.1271	-4.2
		$C13H16NO2^+$	218.1176	218.1165	-5.0
		$C12H14NO^+$	188.1070	188.1059	-5.8
		$C10H9O2^+$	161.0597	161.0586	-6.8
		$C5H12N^+$	86.0964	86.0961	-3.4
E-M1	8.7	C12H17NO3	224.1281	224.1276	-2.2
		$C12H16NO2^+$	206.1176	206.1174	-0.9
		$C12H14NO^+$	188.1070	188.1072	1.0
		$C5H12N^+$	86.0964	86.0968	4.6
E-M2	15.3	C11H13NO3	208.0968	208.0966	-0.4
		$C11H12NO2^+$	190.0863	190.0857	-3.4
		$C10H10NO+^+$	160.0757	160.0764	4.2
		$C8H5O3^+$	149.0233	149.0227	-1.2
		$C9H10N^+$	132.0808	132.0809	1.2
E-M3	17.4	C13H19NO3	238.1438	238.1428	-3.7
		$C13H18NO2^+$	220.1332	220.1337	2.2
		$C11H13NO2^+$	191.0940	191.0944	2.1
		$C10H9O^+$	145.0648	145.0636	-8.2
		$C8H7O2^+$	135.0441	135.0438	-2.2
		$C6H12N^+$	98.0964	98.0967	3.0
Dibutylone	17.7	C13H17NO3	236.1281	236.1280	-0.4
		$C11H11O3^+$	191.0703	191.0704	0.5
		$C10H9O2^+$	161.0597	161.0596	-0.6
		$C8H5O3^+$	149.0233	149.0232	-0.6
		$C5H12N^+$	86.0964	86.0967	3.4
D-M1a	8.5	C12H17NO3	224.1281	224.1274	-3.1
		$C10H9O2^+$	161.0597	161.0597	0.0
		$C9H11O2^+$	151.0754	151.0752	-1.3
		$C7H5O3^+$	137.0233	137.0231	-1.4
		$C7H7O2^+$	123.0441	123.0437	-3.2
		$C5H12N^+$	86.0964	86.0966	2.3
D-M1b	16.2	C12H17NO3	224.1281	224.1287	2.7
D-M2	15.3	C11H13NO3	208.0968	208.0974	2.9
D-M3	16.7	C12H15NO3	222.1125	222.1127	1.3
		$C12H14NO^+$	204.1019	204.1021	1.0
		$C11H12NO^+$	174.0913	174.0915	0.7
		$C10H9O2^+$	161.0597	161.0603	3.8
		$C10H12N^+$	146.0964	146.0967	1.5
D-M4	17.2	C13H19NO3	238.1437	238.1417	-8.3
		$C13H18NO2^+$	220.1332	220.1329	-1.3
		$C11H13NO2^+$	191.0940	191.0933	-3.7
		$C10H9O^+$	145.0648	145.0647	-0.6
		$C8H7O2^+$	135.0441	135.0435	-4.4
D-M5	22.8	C13H17NO4	252.1230	252.1236	2.4
		$C10H9O3^+$	177.0546	177.0558	6.8
		$C8H5O3^+$	149.0233	149.0231	-1.3
		$C5H12N^+$	86.0964	86.0965	1.1

Table 1. Continued.

Name	RT	Proposed elemental composition	Exact mass $[M+H]^+$	Measured mass $[M+H]^+$	Error (ppm)
Dimethylone	13.1	C12H15NO3	222.1125	222.1121	-1.8
		$C10H9O3^+$	177.0546	177.0542	-2.2
		$C9H7O2^+$	147.0441	147.0438	-2.0
		$C4H10N^+$	72.0808	72.0810	2.7
M-M1	5.4	C11H15NO3	210.1124	210.1124	0.0
		$C9H9O3^+$	165.0546	165.0565	11.5
		$C9H7O2^+$	147.0441	147.0451	6.8
		$C8H9O2^+$	137.0597	137.0586	-8.0
		$C4H9O2^+$	89.0597	89.0595	-2.2
		$C4H10N^+$	72.0808	72.0806	-2.7
M-M2	11.8	C11H13NO3	208.0968	208.0967	0.4
		$C11H12NO2^+$	190.0863	190.0855	-4.4
		$C10H10NO^+$	160.0757	160.0753	-1.4
		$C9H7O2^+$	147.0441	147.0433	-5.7
		$C9H10N^+$	132.0808	132.0808	0.0
M-M3	12.3	C12H17NO3	224.1281	224.1273	-3.5
		$C12H16NO2^+$	206.1176	206.1171	-2.4
		$C11H13NO2^+$	191.0940	191.0933	-3.7
		$C9H7O^+$	131.0491	131.0490	-0.7
M-M4	18.0	C12H15NO4	238.1073	238.1073	0.0
		$C13H8N^+$	178.0651	178.0624	-15.2
		$C8H5O3^+$	149.0233	149.0248	10.0
		$C4H10N^+$	72.0808	72.0808	0.0

The ion at *m/z* 160 was generated by the further loss of a dioxolane, respectively. The ion at *m/z* 149 resulted from the loss of the amine group moiety. The ion at *m/z* 132 resulted from the loss of a dioxolane, then following demethylation and reduction. The MS spectrum of E-M3 displayed major product ions at *m/z* 220, 191, 145, 135, and 98. The ions at *m/z* 220 and 135 indicated the loss of water and amine group moiety, respectively. The ion at *m/z* 191 was generated by the further loss of water from the ion in the demethylated form of the parent and then the formation of a radical. The ion at *m/z* 98 resulted from the loss of a 1,3-benzodioxole group.

In vitro metabolism of dibutylone in human liver microsomes

The incubation of dibutylone with pooled human liver microsomes in the presence of an NADPH-generating system generated six metabolites (Figure S1, B). Their $[M+H]^+$ ions were observed at *m/z* 224 for D-M1a and D-M1b by demethylenation, *m/z* 208 for D-M2 by di-demethylation, *m/z* 222 for D-M3 by demethylation, *m/z* 238 for D-M4 by reduction and *m/z* 252 for D-M5 by N-oxidation, respectively. Metabolites D-M1b and D-M4 were found in previous studies. The accurate mass data for the product ions of the metabolites are summarized in Table 1.

The MS/MS analysis of protonated dibutylone yielded a major product ion at *m/z* 191, 161, 149, and 86 (Figure S3). The ion at *m/z* 191 resulted from the deamination of dibutylone and the subsequent loss of alkylation resulted in the generation of the ion at *m/z* 149. The ions at *m/z* 161 generated the loss of water and methylation, and that at *m/z* 86 was formed by alpha-cleavage between the 1 and 2 positions. D-M1 was observed to have a retention time of 8.5 min with a protonated ion at *m/z* 224. The molecular weight of D-M1 was 12 Da lower than that of dibutylone. The MS/MS of the protonated D-M1 generated major product ions at *m/z* 161, 151, 137, 123, and 86. The ions at *m/z* 137 and 86 resulted from the alpha-cleavage between positions 1 and 2. The product ion at *m/z* 161 generated the loss of the amine group and the oxidation and subsequent loss of alkylation resulted in the generation of the ions at *m/z* 151 and 123. D-M2 was observed to have a retention time of 15.3 min, with an $[M+H]^+$ ion at *m/z*

208. The protonated D-M2 was 28 Da lower than that of dibutylone, suggesting that this metabolite was the di-demethylation derivative of dibutylone. However, MS/MS of D-M2 was not generated due to low intensity of metabolite. D-M3 was observed to have a retention time of 16.7 min, with an $[M+H]^+$ ion at *m/z* 222. The protonated D-M3 was 14 Da lower than that of dibutylone, suggesting that this metabolite was the demethylation derivative of dibutylone. The MS/MS spectra of protonated D-M3 showed major product ions at *m/z* 204, 174, 161, and 146. The characteristic product ion at *m/z* 204 resulted from dehydration. The ions at *m/z* 174 resulted from the loss of the dioxolane. The ion at *m/z* 161 was formed by following the deamination and demethylation by reduction. The product ion at *m/z* 146 was formed by the loss of dioxolane, demethylation, and then reduction. D-M4 was observed to have a retention time of 17.2 min with an $[M+H]^+$ ion at *m/z* 238. The protonated D-M4 was 2 Da higher than that of dibutylone, indicating that this metabolite was the hydrogenated derivative of dibutylone. MS/MS spectra showed a major product ion at *m/z* 220 resulting from the loss of water and *m/z* 135 indicated the loss of the amine group and the alkylation group moiety. The ion at *m/z* 191 was generated by the further loss of water from the ion in the demethylated form of the parent and then the formation of radicals. D-M5 was observed to have a retention time of 22.8 min, with an $[M+H]^+$ ion at *m/z* 252. The protonated D-M5 was 16 Da higher than that of dibutylone, suggesting that this metabolite was the N-oxide derivative of dibutylone. The MS/MS spectra of protonated D-M5 showed major product ions at *m/z* 192, 177, 149, 135, 86, and 60. The characteristic product ion at *m/z* 192 resulted from the loss of the amine group. The ions at *m/z* 177 and 149 resulted from the loss of the amine and alkyl groups, and following the loss of the keto group was the *m/z* 135 ion. The ion at *m/z* 86 was formed by alpha-cleavage between the 1 and 2 positions. The product ion at *m/z* 60 was formed by an N-oxide fragment ion.

In vitro metabolism of dimethylone in human liver microsomes

The incubation of dimethylone with pooled human liver microsomes in the presence of an NADPH-generating system generated four metabolites (Figure S1, C). Their $[M+H]^+$ ions were observed at *m/z* 210 for M-M1 by demethylenation, m/z 208 for M-M2 by dealkylation, *m/z* 224 for M-M3 by demethylenation, and *m/z* 238 for M-M4 by hydroxylation, respectively. Metabolite M-1 was found in previous studies. The accurate mass data for the product ions of the metabolites are summarized in Table 1.

The MS/MS analysis of protonated dimethylone yielded major product ions at *m/z* 177, 147, and 72 (Figure S4). The ion at *m/z* 177 resulted from the deamination of dimethylone, and the subsequent loss of methyl and oxidation resulted in the generation of the ion at *m/z* 147. The ions at *m/z* 72 were formed by alpha-cleavage between the 1 and 2 positions. M-M1 was observed to have a retention time of 5.4 min, with a protonated ion at *m/z* 210. The molecular weight of M-M1 was 12 Da less than that of dimethylone. The MS/MS of protonated M-M1 generated major product ions at *m/z* 165, 147, 137, 89, and 72. The ions at *m/z* 165 and 72 resulted from alpha-cleavage between positions 1 and 2. The ion at *m/z* 147 resulted in a loss of the keto and amine groups following the ring. The ion at *m/z* 137 generated the loss of the amine group and oxidation. The ion at *m/z* 89, found only in M-M1, resulted from the cleavage of the benzene ring. M-M2 was observed to have a retention time of 11.8 min, with an $[M+H]^+$ ion at *m/z* 208. The protonated M-M2 was 14 Da less than dimethylone, indicating that this metabolite resulted from the dealkylation. The MS/MS spectra of protonated M-M2 showed major product ions at *m/z* 190, 160, 147, and 132. The ion at *m/z* 190 indicated dehydration. The ion at *m/z* 160 was generated by the loss of dioxolane. The ion at *m/z* 147 resulted from the loss of amino group moiety and reduction. The ion at *m/z* 132 was formed by the loss of dioxolane and reduction. M-M3 was observed to have a retention time of 12.3 min, with an $[M+H]^+$ ion at *m/z* 224. The protonated M-M3 was 2 Da higher than dimethylone, indicating that this metabolite was the reduced derivative of dimethylone. The MS/MS spectra showed a major product ion at *m/z* 206 resulting from the loss of water, and *m/z* 131 indicated the loss of dioxolane moiety. The ion at *m/z* 191 was generated by the further loss of water from the ion in the demethylated form of the parent and then the formation of a radical. M-M4 was observed to have a retention time of 18.0 min, with an $[M+H]^+$ ion at *m/z* 238. The protonated M-M4 was 16 Da higher than dimethylone and was eluted later than the parent, indicating that this metabolite can be postulated to be the N-oxide derivative of dimethylone. The MS/MS spectra of protonated M-M4 showed major product ions at *m/z* 178, 149, 72, and 60. The ion at *m/z* 60 was only found in the N-oxide metabolite fragment ion spectrum. The ions at *m/z* 178, 149, and 72 were observed in other metabolites.

Discussion

In this study, the metabolism of eutylone, dibutylone, and dimethylone was investigated based on accurate mass and MS/MS product ion analyses. The metabolism pathways of them are proposed in Figure 1. The synthetic cathinones included in this study recently became available worldwide. Eutylone, dibutylone, and dimethylone have common metabolites through *O*-demethylenation and the reduction of the keto function in human liver microsomes. N-oxide metabolites were detected only in the reaction samples with dibutylone and dimethylone, which are tertiary amines. The major metabolism of these synthetic cathinones is *O*-demethylenation.

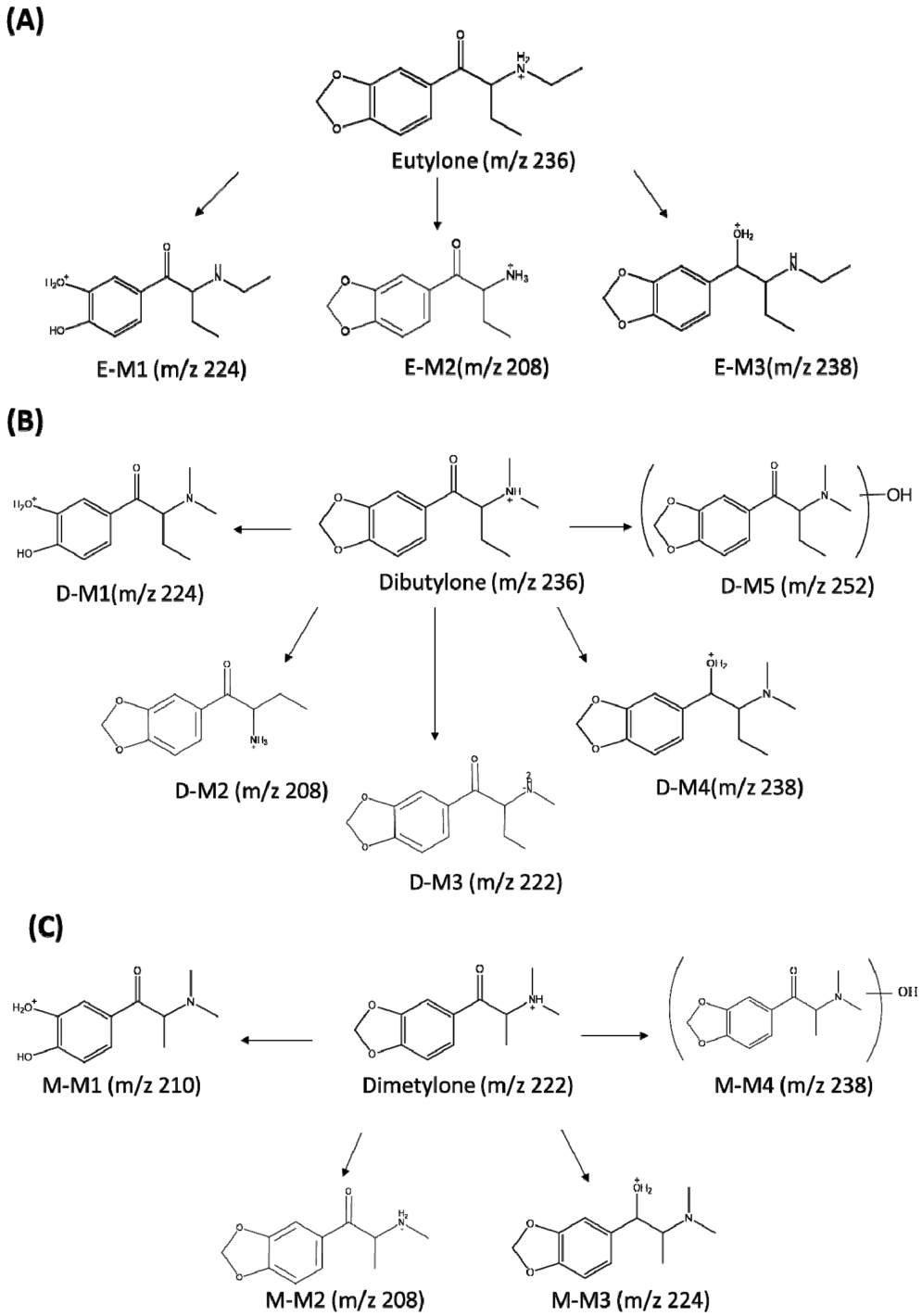

Figure 1. Proposed metabolic pathways of (A) eutylone, (B) dibutylone, and (C) dimethylone.

Compared with reported data, metabolites through demethylenation, demethylation, and hydrogenation were equally identified.[17-19] However, hydroxylation metabolites reported in previous reports were not identified, and the N-oxide metabolites were identified in this study, newly. The reason why the hydroxylation metabolites did not appear in this study was expected that as the pretreatment methods of samples were different, they were lost in the intermediate process such as solid phase extraction, and were not analyzed. From another point of view, in the case of hydroxylation and N-oxide metabolites, there was a possibility that the chemical formula shift is the same and

therefore they could be recognized same metabolites. However, in this study, considering the RT shift of each metabolite with the parent molecule, N-oxide, not hydroxylation, was reasonably judged, and MS/MS fragmentation was also confirmed. Thus, N-oxide metabolites were expected to be generated and further confirmation is needed about hydroxylation metabolites.

Representative compounds of synthetic cathinones include 3,4-methylenedioxymethamphetamine (MDMA) and mephedrone. Meyer et al. and Lim et al. published a metabolism study of MDMA.[10,11,14] MDMA is metabolized through two main pathways. The first is the *O*-demethylenation of the ring followed by methylation, glucuronidation, or sulfatation. The other is the *N*-dealkylation to 3,4-methylendioxyamphetamine (MDA), followed by the oxidation to benzoic acid derivatives. A major metabolism in the human samples was *O*- demethylenation followed by methylation.[10,11,14] The synthetic cathinones investigated in the present study as well as MDMA have common methylenedioxy groups. According to the results, *O*-demethylenation is a major metabolic pathway in synthetic cathinones with methylenedioxy groups.

The metabolism of mephedrone was investigated in human urine samples.[16] Mephedrone was metabolized to yield six Phase I and four Phase II metabolites. The Phase I reactions were *N*-demethylation, a reduction of the keto function, hydroxylation in C_3 and in the benzylic carbon, and the oxidation of C_3 and benzylic methyl into a carboxylic acid. Phase II metabolism occurred mainly via conjugation with glucuronic acid and succinic acid. The synthetic cathinones investigated in the present study as well as mephedrone have common beta-keto function groups. Pozo et al. reported that mephedrone with a ketone group metabolizes to a reduced form. The fragment feature of this metabolite was the loss of water at the most abundant peak in the spectrum, and the subsequent losses of CH_3 and methylamine.[16] The methylenedioxy designer drugs used in this study generated reduced forms of metabolites that exhibited fragment ions through the loss of water, as well as the subsequent losses of CH_3 and methylamine, as shown in the mephedrone metabolite.

Conclusion

This study focused on the metabolism of the newly abused designer drugs eutylone, dibutylone, and dimethylone. The investigation of the metabolism patterns of these methylenedioxy drugs was similar to that of previously reported synthetic cathinones. Demethylenation of the dioxolane group and hydroxylation are common metabolic pathways for most methylenedioxy designer drugs. This information could provide evidence for the *in vivo* metabolism of methylenedioxy designer drugs in biological samples, and would be helpful in appropriate biomarker development for detecting drug use. At this time, information on the metabolism of methylenedioxy designer drugs is limited especially for humans, and further studies are needed to clarify their properties.

Supporting information

Supplementary information is available at https://docs.google.com/document/d/1-qHDmTj4hWzTzvjMpmwHuMg-hLe7r-1G/edit?usp=sharing&ouid=111353140014732050956&rtpof=true&sd=true

Acknowledgements

This work was supported by the National Research Foundation of Korea (NRF) grant by the Korea government (NRF-2021R1A2C1010428).

References

1. Kalix, P. *Pharmacol Toxicol* **1992**, 70, 77. https://doi.org/10.1111/j.1600-0773.1992.tb00434.x.
2. Al-Motarreb, A.; Al-Habori, M.; Broadley, K.J. *J Ethnopharmacol* **2010**, 132, 540. https://doi.org/10.1016/j.jep.2010.07.001.
3. Karila, L.; Reynaud, M. *Drug Test Anal* **2011**, 3, 552. https://doi.org/10.1002/dta.210.
4. Baumann, M.H.; Ayestas, M.A., Jr.; Partilla, J.S.; Sink, J.R.; Shulgin, A.T.; Daley, P.F.; Brandt, S.D.; Rothman, R.B.; Ruoho, A.E.; Cozzi, N.V. *Neuropsychopharmacology* **2012**, 37, 1192. https://doi.org/10.1038/npp.2011.304.
5. Kalant, H. *CMAJ* **2001**, 165, 917.
6. Baumann, M.H.; Partilla, J.S.; Lehner, K.R.; Thorndike, E.B.; Hoffman, A.F.; Holy, M.; Rothman, R.B.; Goldberg, S.R.; Lupica, C.R.; Sitte, H.H.; Brandt, S.D.; Tella, S.R.; Cozzi, N.V.; Schindler, C.W. *Neuropsychopharmacology* **2013**, 38, 552. https://doi.org/10.1038/npp.2012.204.
7. Marusich, J.A.; Antonazzo, K.R.; Wiley, J.L.; Blough, B.E.; Partilla, J.S.; Baumann, M.H. *Neuropharmacology* **2014**, 87, 206. https://doi.org/10.1016/j.neuropharm.2014.02.016.
8. Staack, R.F.; Maurer, H.H. *Curr Drug Metab* **2005**, 6, 259. https://doi.org/10.2174/1389200054021825.
9. Kim, I.S.; Rehman, S.U.; Choi, M.S.; Jang, M.; Yang, W.; Kim, E.; Yoo, H.H. *J Pharm Biomed Anal* **2016**, 131, 160. https://doi.org/10.1016/j.jpba.2016.08.025.
10. Lim, H.K.; Foltz, R.L. *Chem Res Toxicol* **1988**, 1, 370. https://doi.org/10.1021/tx00006a008.
11. Lim, H.K.; Foltz, R.L. *Chem Res Toxicol* **1989**, 2, 142. https://doi.org/10.1021/tx00009a002.
12. Pickering, H.; Stimson, G.V. *Addiction* **1994**, 89, 1385. https://doi.org/10.1111/j.1360-0443.1994.tb03734.x.
13. Griffiths, P.; Mravcik, V.; Lopez, D.; Klempova, D. *Drug Alcohol Rev* **2008**, 27, 236. https://doi.org/10.1080/09595230801932588.
14. Meyer, M.R.; Peters, F.T.; Maurer, H.H. *Drug Metab Dispos* **2008**, 36, 2345. https://doi.org/10.1124/dmd.108.

021543.
15. Antolino-Lobo, I.; Meulenbelt, J.; Nijmeijer, S.M.; Scherpenisse, P.; van den Berg, M.; van Duursen, M.B. *Drug Metab Dispos* **2010**, 38, 1105. https://doi.org/10.1124/dmd.110.032359.
16. Pozo, O.J.; Ibanez, M.; Sancho, J.V.; Lahoz-Beneytez, J.; Farre, M.; Papaseit, E.; de la Torre, R.; Hernandez, F. *Drug Metab Dispos* **2015**, 43, 248. https://doi.org/10.1124/dmd.114.061416.
17. Yeh, Y.L.; Wang, S.M. *Drug Test Anal* **2022**, 14, 1325. https://doi.org/10.1002/dta.3258.
18. Krotulski, A.J.; Mohr, A.L.A.; Papsun, D.M.; Logan, B.K. *J Anal Toxicol* **2018**, 42, 437. https://doi.org/10.1093/jat/bky022.
19. Mohr, A.L.; Friscia, M.; Logan, B.K. *Washington, DC: US Department of Justice* **2016**.

